The Nucleus ***54****, No. 2 (2017) 97-104*

www.thenucleuspak.org.pk

The Nucleus

ISSN 0029-5698 (Print)

ISSN 2306-6539 (Online)

Fatigue Life Estimation of TIG Welded Aluminum Alloy (Aa2219) Under Combined Loading

A. Shahzadi*, G.Y. Chohan, Mudaser Ullah and Q. Ali

Department of Mechanical Engineering, UCET, Sargodha, Pakistan

ashahzadi45@gmail.com,yasin.chohan@uos.edu.pk,engr.mudaser.phd@gmail.com,mirzaqasimali@gmail.com

ARTICLE INFO

Article history :
Received : 13 February, 2017
Accepted : 14 June, 2017
Publsihed: 30 June, 2017

Keywords:
Thermal cycling
Fatigue life prediction
S-N curves
Al alloy
FCGR
Microstructure

ABSTRACT

Fatigue life of structural components is greatly influenced by increase in temperature. It is therefore important to study the behavior of materials under Combined Thermal Cycling (CTC). Components and parts made from aluminum are subjected to cyclic loading under high operational temperatures; hence it is necessary to determine fatigue behavior of aluminum alloys under such conditions. In this study crack initiation and fatigue life of aluminum alloy is investigated under four point rotating bending fatigue test at high temperature. CTC and notch geometry effects were also investigated in this study. High temperature testing fixture was developed and installed on the machine to carry out tests at higher temperatures. S-N curves obtained in this study shows that the fatigue life of subjected aluminum alloy is low at higher temperatures. A detailed investigation on microstructure was also made and used to show harmonious experimental results.

1. Introduction

Due to good strength to weight ratio Aluminum is extensively used in automobile, aerospace and construction industry. Yet, commercially produced aluminum components may contain notches or holes which act as stress risers when load is applied on these components. Another important consideration is that these components do not always operate at room temperature. Cyclic mechanical loading on such components at higher temperatures might cause them to fail well before anticipated life causing failure of component. Hence, it is necessary to investigate the fatigue life of aluminum alloys under Combined Thermal Cycling & Mechanical loading(CTC&ML).

It is important to underline the historical advancements with respect to fatigue. In the late 1840s an observation was made that the shoulders of railroad axles frequently failed. A German scientist Wohler [1] performed many experiments involving cyclic loads on components. This experiment which was carried out to investigate the failure in railway axles was the first systematic study in the history of fatigue. Using S-N curves, he depicted that below a certain stress limit the material doesn't fail while with increasing stress its life decreases. Hence, Wholer is considered as the father of fatigue testing. His work also emphasized how stress range is more important than actual value of stress on a component. Gerber [2] his research to find out the effect of mean stress on fatigue life while, Goodman presented a simplified model for Gerber's work. Ewing and Humfrey [3] used optical microscope in the early 20th century to discover when the phenomena of fatigue failure occurs. Slip lines and bands formation due to repetitive loadings were observed for the first time. Griffith [4] in the 1920s gave astounding numerical model for crack propagation and backed it with his experimental work on brittle glass specimens. Gassner in 1939 emphasized the value of variable amplitude load testing. Block testing method was popular until servo hydraulic systems became available to carry out more precise cyclic loading fatigue tests by 1960. Strain-controlled low-cycle fatigue testing became popular when Manson [5] linked the plastic strain applied on the material to its fatigue life. Elbert in 1970 proved the importance of crack closure on Fatigue Crack Growth Rate. By providing this model he laid the foundations of modern developments in understanding and quantifying fatigue crack growth rate. Paris in 1970 did extensive experimental work to demonstrate that a threshold stress intensity factor could be obtained for a specific material. In the late 20th century many researchers started working to investigate the complex behavior of materials under fatigue loading. Stephens [6] gave the idea that structures and machines undergo diverse loading conditions. These loadings may be simple and harmonic or totally random.

Ranc [7] carried out their research on high yield strength steels under Very High Cycle Fatigue and found out that in such materials failure occurs on sub surface rather than on the surface. Such kind of failure initiation is called "fish eye". Ultrasonic fatigue testing on two

*Corresponding author

different bearing steel samples was conducted by Akiniwa [8]. The S-N curves obtained for both samples were different because of the difference in size of precipitates. Leidmark [9] presented the fatigue crack imitation in a notched single-crystal super alloy component.

Lazzarin [10] investigated the crack initiation and crack propagation in deep drawn plates and wrought aluminum sheets. The V and U-shape notches were developed to be the basis of characterization of plates, radius of notch root in specimens ranged from 0.1-10 mm, depth of notch was 10mm and the thickness of plate was 2mm for light alloy and for steel it was 5mm. Both specimens were tested under similar loading conditions and the effect of different notches was studied in this research. Makkonen [11] found out the effect of geometric size on the fatigue life of samples. Linear Elastic Fracture Mechanics can be used to find the probability of crack initiation as, greater the specimen size, the more is the probability of cracking. Hsu [12] investigated the fatigue crack propagation effects in samples under compression-compression loading conditions. Tzu-Yin presents the initiated cracks in ductile materials. It can be observed that in such material, crack initiate at 45 degree angle because of excessive plastic deformation [12]. Whereas, the materials which possess more brittle behavior, have cracks initiate in direction perpendicular to loading axis. Roth [13] worked on the fatigue life of stainless steel AISI-304L. They found that small cracks initiate very close to the specimen boundaries width 70% locality. Such cracks could be observed when 5% of total fatigue life had passed. As a result so many slip planes are generated and give rise to crack initiation. Thomas Hansson & K.J. Miller work is related to the current research work. Yet there are still many parameters which are need to be addressed. K.J. Miller work which is discussed later in detail addresses the investigation of crack initiation phase which was investigated experimentally. After this crack propagation behavior under CTC & ML was investigated by K.J. Miller. The tests were carried out at 1 Hz with temperature varying between 170 to 570^{o}C using induction heating system. The data was obtained by change in step's of 20^{o}C. It was reported that the fatigue crack propagation rate is drastically affected because of change in working temperature ranges.

The prediction of fatigue crack initiation and propagation has become easier because of the involvement of computational methods. In computing technology especially Computer Aided Engineering involves the simulations of both kinds, static and dynamic of the desired material. These simulations are based on finite element analysis codes. With the help of these subroutines or coding it has become easily accessible to estimate the fatigue life of different parts. There is another advantage for designer that they can predict failure cycles while developing structures and machines at a fast pace [6].

In this research an infrared sensor was installed on the machine with a slit disc passing through it. The LCD shows the cycle count. Thermal Loading is provided by the electric rod. A well calibrated temperature measurement module of an advanced millimeter was used for measuring the surface temperature of the sample during experiments. Specially machined sheets of Graphite Iron were used as a shield on the bearings to protect them from heating. A packing sheet was inserted between the motor and the specimen to prevent the specimen from forced draft cooling effect, caused by the forced draft fan of the motor to keep the motor body cool. In this paper concept is developed to understand and estimate the fatigue life of Tungsten Inert Gas welded Al alloy under combined loading.

2. Experimental Work

AA2219 Aluminum grade which is used to manufacture structural components was tested in this work. The chemical composition of the material was tested using mass spectrometer. Chemical composition of AA2219 is show in Table 1.

Table 1: Chemical composition of alloy

Elt	Al	Cu	Si	Fe	Mn	Mg
%	>93.8	6.3	0.2	0.3	0.4	0.02
Elt	Zn	Zr	V	Residuals	Sn	Ti
%	0.1	0.25	0.15	0.15	0.02	0.10

For preparation of specimen raw material for the sample was graded AA2219 Rods of 20mm diameter, procured from the market. Standard testing size and geometry of the 4 point rotating bending fatigue test samples has been presented in literature. Two parameters of the samples are of consideration:

1. Specimen Length
2. Specimen Diameter

Specimens of 17mm outer dia. and 226 mm length were used during testing. Specimens were reduced to 12mm dia. from centre as per standard. In the middle a notch of 0.75mm depth and grove angle of 60˚ is introduced to localize the stresses. Hence the dia. of the sample from centre is 10.5mm.

The specimen was machined on a manual lathe and ground to achieve accurate geometry. Drawing of the sample is presented in Fig.1.Special consideration was given to the neck of the specimen to make sure that it is scratch free and well-polished. A 60^{o} threading tool was used to machine the notch at the centre of the specimen. Rotating bending machine was used for experiments.

PQ-6 rotating bending fatigue testing machine shown in Fig. 2 is simple and easy to operate and has, good stability and reliability. It is used to investigate the S-N curves and endurance limits of wide variety of materials. PQ-6 is a machine with all the switches and safeties installed. Once started it automatically counts the number of cycles and comes to a halt when specimen fails. For the preparation of the specimen for microstructure evaluation the filler material used is AA2319, which is the recommended filler material for TIG welding of this alloy. In this research internal temperature was more than 30^0C in the case of CTC, and load varies from 160 to 250N. In phase I experiments load remains constant till failure.

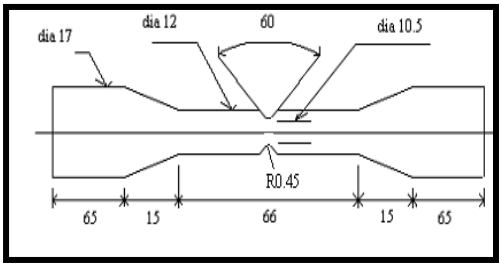

Fig. 1: Dog bone Specimen

Fig. 2: Rotary bending fatigue testing

An artificial heating environment was created by an electric rod of 1000W. It was fixed on the specimen with the help of a stand as shown in Fig. 3. It was observed during all experiments that air from the motor fan was going to the specimen and causing the specimen to cool. A packing sheet was prepared according to the parameters of the machine was fitted on the machine to stop the air from the motor's fan reaching the specimen. All the metal strips on the stand were properly insulated by insulation paint. This was done to prevent from electric shocks.

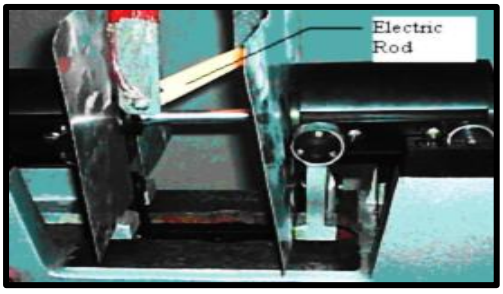

Fig. 3: Heating of the specimen

The thermal loading was added with ML and results were observed. During experiments the temperature of the upper notch root and lower notch root was 90-100^0C and 60-70^0C respectively while the cross sectional temperature was 55-60^0C. In phase II load varied during experimentation and in phase III TL was added with ML, where as temperature of notch root remained constant in all phases.

3. Results and Discussion

Research was carried out to discover the initiation of crack and failure in aluminum at constant but fully reversible loading. Tests were carried out at room temperature and at almost 100^oC. All the testes were carried out on single geometry notch. S-N curves and crack initiation curves were plotted to depict the effect of thermal and mechanical loading. It was observed that thermal loading also affected bending moment and equivalent stresses. Load is converted into bending stress by using Eq.1 and to obtain the alternating stress concentration factor is multiplied with bending stress.

$$\sigma = 509.3Q/d3 \quad (1)$$

Stress concentration factor is used to calculate stress at the notch root, and value for Kt is taken as 2.45 according to specimens. Stress Concentration Factor for notch on specimen can be obtained using curves shown in Fig. 4.

From the geometry of specimen, the following parameters can be obtained

D = 12mm; d = 10.5mm; r = 0.45mm; D/d = 1.15;

r/d = 0.04

So using Fig. 4, the value of Kt is approximately estimated as 2.45 against obtained value of r/d = 0.04 [14].

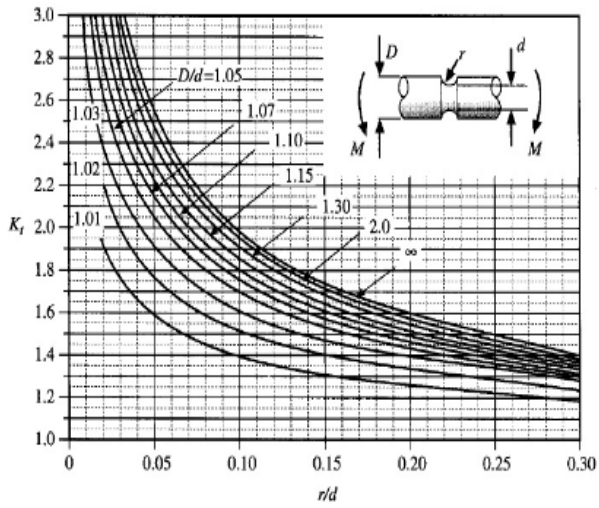

Fig. 4: Different values of K_t VS r/d [14]

In the experiments when only ML is applied on the specimen fatigue life drastically decreases. The S-N curve which is obtained for mechanical loading is shown in Fig. 3.

And when TL is applied with ML, fatigue life of specimen is further decreases which are presented in Table 3 and Fig. 6.

Table 2: Technical specifications of PQ-6

Bending torque (maximum)	6 Kg f. m (60 N.m)
RPM	3000 r/min
Co-axial of left and right claws	0.02 mm
Specimen Diameter	12, 17 mm
Specimen Length	226 mm
Working temperature	≤ 30 C
Maximum counter number	1 x 10^7
Motor specs	0.75 KW, 380V, 50Hz, 3 phases,1.8A
Dimensions	1170 x 500 x 1220 mm
Weight	455 Kg

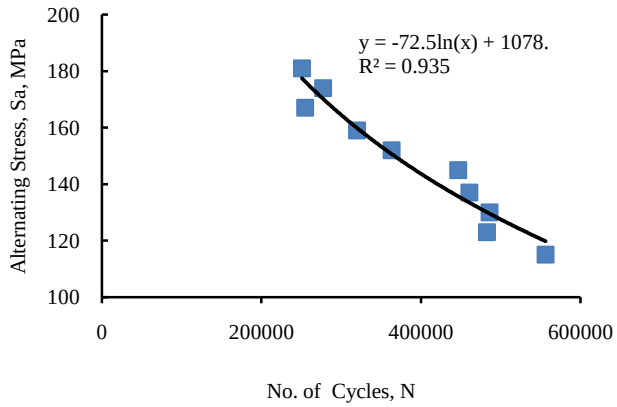

Fig. 5: SN curve with ML only

Table 3: S-N curve data calculation (ML&TL)

No.	Load	Diameter 'd'	σ = 509.3Q/d3 N/mm^2 or Mpa	Alternating stress S_a= σ*k_t	No. of Cycle to Failure
1	160	12	47	115	343593
2	170		50	123	290225
3	180		53	130	221783
4	190		56	137	205241
5	200		59	145	233727
6	210		62	152	150392
7	220		65	159	107103
8	230		68	167	70621
9	240		71	174	64817
10	250		74	181	37932

It can be observed that with increase in stress value the total life of specimen drastically decreases [15-17]. It was also observed that the endurance limit of aluminum was not reached within the applied loading conditions. A comparison of S-N curve is plotted in (Fig. 7) in which the effect of TL is clearly observed.

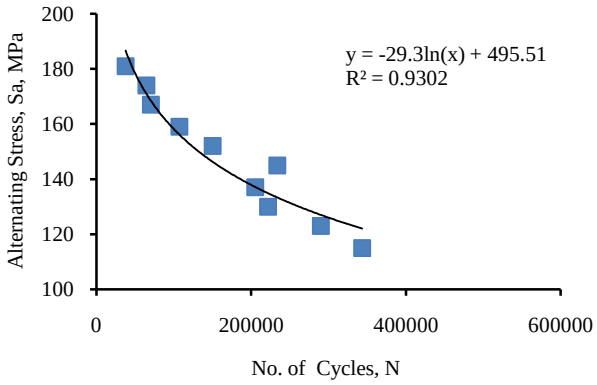

Fig. 6: S-N curve (ML and TL)

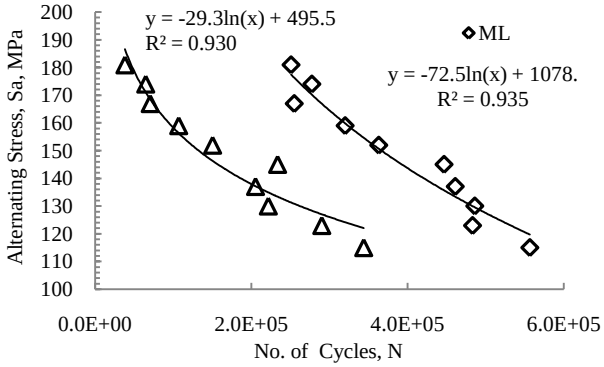

Fig. 7: Comparison of S-N curves

4. Initiation Phase Prediction

Distinguishing the crack initiation phase from crack propagation phase is very important; The cyclic transitions required to initiate crack in specimen and those required to propagate crack in specimen can only be improved if the values are determined exactly [18-20]. During two step experiment, initially low load was applied, and after specific cycles higher load was applied. If high load is applied initially, it causes strain hardening in the material [21-23]. In two step loading, low loading condition is kept for more than half of its total life before applying higher load. It is ensured that crack is already initiated and in propagation phase before applying higher load. The reading for number of cycles is recorded. These numbers of cycles are designated as N_2. After fracture the number of cycles to failure are designated as N_1.

Ni = Cycles to initiate a fatigue crack
Np= Cycles for crack to propagate to final fracture
S2 = Low Load
S1 = High Load
Nf2= Total life at low load
Nf1= Total life at high load
N2 = Number of cycles for S2 in two step loading
N1 = Number of cycles for S1 in two step loading
x= N_2/ N_{f2}
y= N_1/ N_{f1}
z = fraction for low loading

$$\times N_{f2} = N_{i2} + zN_{p2} \quad (2)$$

z = 1 - y

$$y N_{f1} = y N_{p1} \quad (3)$$

$N_{i1} = 0$

$$\times N_{f2} = N_{i2} + (1-y) N_{p2}$$

$$\times N_{f2} = N_{i2} + (1-y) (N_{f2} - N_{i2})$$

$$N_{i2} = N_{f2}(x+y-1)/y \quad (4)$$

Number of cycles required to initiate crack in the specimen can be found using Eq. 4. A total of 7 experiments were carried out under ML to investigate crack initiation cycles. The test was carried out for fully reversed cyclic load applied on Rotating Bending Fatigue Test Machine. N_{f2}& N_{f1} were taken from the previous one step loading tests as discussed earlier. Initiation phase life with respect to different loads (ML only) is shown Fig. 8.

It is clear that without TL the fatigue life of aluminum reduces with increasing ML. A total of 7 experiments were carried out under ML & TL to investigate the crack initiation cycles. The test was carried out for fully reversed cyclic load applied on Rotating and Bending Fatigue Test Machine. N_{f2} & N_{f1} were taken from the previous one step loading tests as discussed earlier. In Fig. 9, the life of initiation phase is shown when specimens are tested under combined loadings.

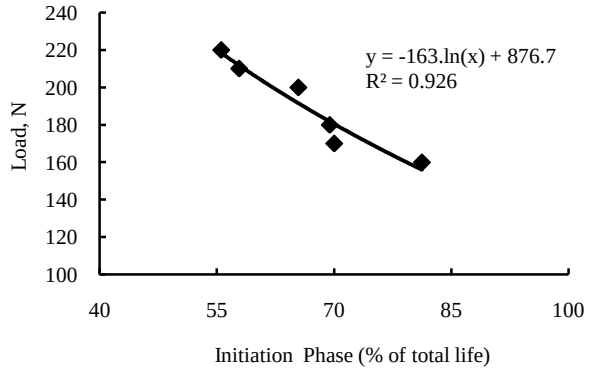

Fig. 8: Effect of loading magnitude on initiation phase duration (ML only)

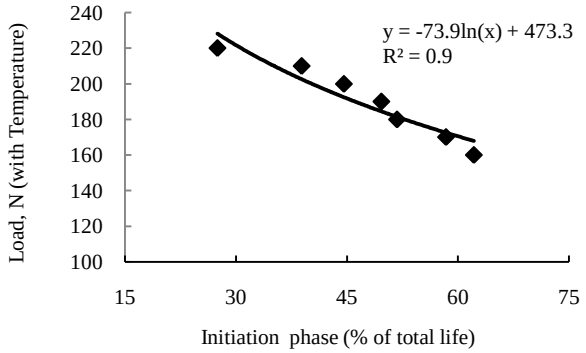

Fig. 9: Effect of loading magnitude on initiation phase duration (ML & TL)

It can be seen that the initiation phase largely depends on the applied load [24] in two step loading and decreases with increasing load. Numbers of cycles required for crack initiation were calculated using Eq. 4 and are presented in Fig. 10. The curves have been plotted together for comparison to better understand the thermal loading effect. During the CTC & ML crack initiation and stage I propagation life is reduces as shown in Fig. 10.

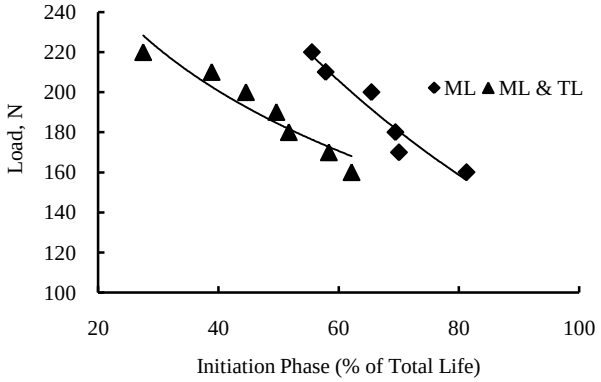

Fig. 10: Comparison of initiation phase curves for different types of loadings

To observe how the collective loading is catastrophic, the least square line fitting theory is used as it is difficult to apply other schemes to picture the shifting behavior of trend lines under combined loading [25-26].

$$Y= ax+b \quad (5)$$

for min. least square errors,

$$\prod = \sum_{i=1}^{n} (Y1 - (a + bXi))2 = \min, \quad (6)$$

For coefficient á & b the least square value should be zero

$$d\prod/d\alpha = 2 \sum_{i=1}^{n} (Yi - (a + bXi)) = 0, \quad (7)$$

By expanding the above eq.

$$\alpha = \frac{(\sum Y)(\sum X2) - (\sum X)(\sum XY) n\pi x}{n\sum x2 - (\sum x)2} \quad (8)$$

Where "α" is determined for both the competitive curves in the same graph and difference in their values is achieved. The expression achieved in Eq. 6 is determined for both loading situations then it is easily obtainable to get the percentage shifting of curve of CTC & ML with respect to the competitive one.

5. Microstructure Development

It has been concluded by many pervious researchers that the mechanical properties are largely affected by the size of primary grain in solid solution alloys. The pure alloys which were specifically used in the current research must possess small and homogeneous grain structure to exhibit best mechanical properties.

5.1 Base Metal (BM)

Aluminum copper phase diagram for AA2XXX base metal alloys is shown in Fig. 11. Dissolved Copper in FCC lattice structured α-Al makes up the alloy.

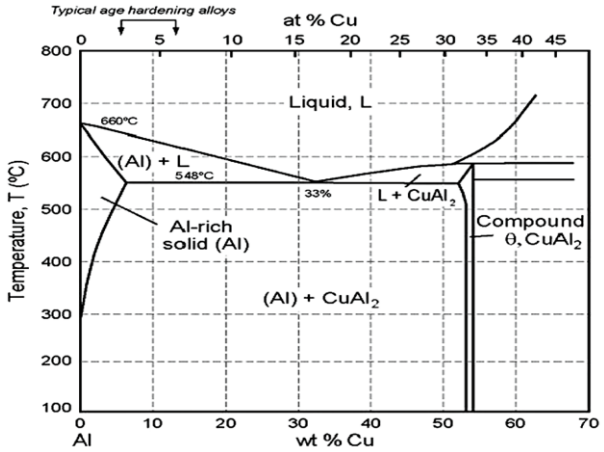

Fig. 11: Al–Cu phase diagram

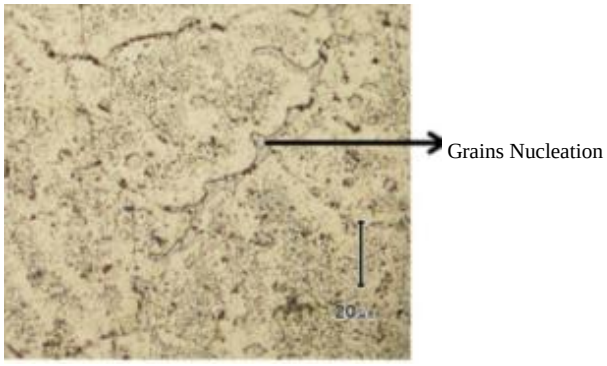

Fig. 12: Grain structure of base metal

T-87 process of heat treatment process was used to further enhance the mechanical properties of the alloys. Because of this heat treatment the inter metallic Al_2Cu (53 wt%) which has circular and asymmetrical shapes (a = 6.06 Å, c = 4.87Å) disperses in grains. This dispersion can be clearly observed in Fig. 12. Second phase alpha particles are randomly scattered on the grain boundaries of round and elongated grains in base metal. Precipitate free zones (PFZ) can also be observed in much less ratio. This happens due to the escape out of inter metallic from grains. PFZ shows that certain ageing phenomena of the base metal has already taken place. Base metal is hardened due to the presence of precipitates yet the porosities, cavities and defective grain boundaries weaken the material and are good sites for material failure, which may occur because of material failure under fatigue cracking or stress corrosion induced cracking.

It was observed that the precipitates hardened the base metal and also provide porosities and cavities on the grain boundaries which act as stress concentration zones when load is applied and it is suspected that material will start failing from these sites.

5.2 Heat-Affected Zone (HAZ)

This is the area which doesn't melt during welding process but due to excessive heating its composition is drastically affected. Heat of welding torch forms supersaturated solution nearby but as the specimen cools down, copper stars to migrate toward the FZ and results in Cu-depleted α-solid phase. Due to depletion of inter metallic in this zone, this is considered to be the most fragile zone. The microstructure is shown in Fig. 13. Because of normalized cooling of HAZ and deficiency of intermetallic bunches of small-size almost equiaxed grains form. Copper settles at grain boundaries making them thick and they seem to be detached from each other, this detachment finally results in degradation of mechanical properties of this zone.

5.3 Fusion Zone (FZ)

Solidified dendritic micro structure is observed to be present in FZ, as depicted in Fig 14. Due to excessive heating during welding, a molten pool forms, because welding solidifies quickly, therefore a provisional meta stable state (Liquid+α) appears as liquidus and solidus. On the other hand, point at which the alloying elements have maximum solubility, second-phase particles θ (Al_2Cu) start precipitating around solidified α-grains.

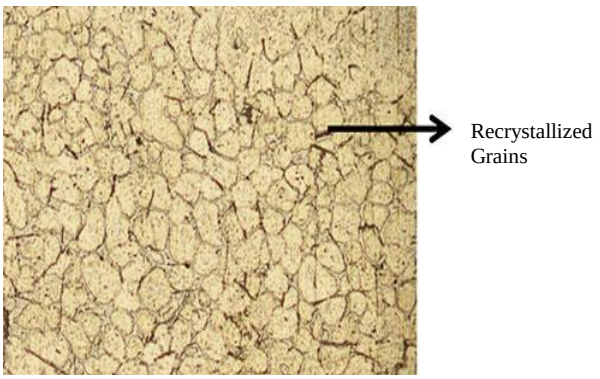

Fig. 13: HAZ of AA2319 filler welded base metal

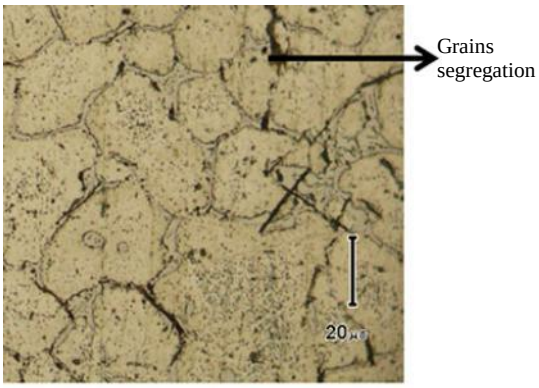

Fig. 14: Microstructure of FZ

Copper concentration in BM and filler metal is 6.3%, and lowers the solvus limit. "α" & "θ" phase at once get separated from each other which is the main reason of degradation of mechanical strength in these zones. Two metastable phases of 2nd phase particles θ" (Al_2Cu) and θ' (Al_2Cu) generate at this stage due to successive cooling [27]. After further cooling to room temperature, the microstructure is as shown in Fig. 14. It can be observed that around denderetic structure and eutectic network is formed. The solidification step always starts from the nucleation of grain which eventually leads to the denderetic structure in FZ. Cavities and voids in FZ are formed due to entrapped gasses or the detachment of denderetic arms; These defects are the main cause of fatigue cracking failure or stress corrosive crack initiation [28]. It was observed by previous researchers that arm spacing in dendrites which are present in FZ is abridged after TIG welding when AA2319 is used as filler metal.

6. Conclusion

1. Number of cycles required for crack initiation decrease with increase in mechanical load.
2. Addition of thermal load with mechanical load during testing further decreases the number of cycles required for crack initiation.
3. Addition of thermal loading also decreases the number of cycles required for final failure.
4. Thermal loading does not affect the deflection in the specimen, which is caused by the mechanical loading
5. Cracks initiate and propagate from the produced notch in the specimen.
6. For the tested loads aluminum doesn't show the endurance limit in the produced S-N curves.
7. Total fatigue life of material is greatly affected by the applied stress value. The life decreases drastically as the load increases.
8. Application of TL causes the mature randomness in second phase particles (Al_2Cu) due to which considerable amount of fatigue life reduction is observed.
9. Migration of Cu from θ particles as well as supersaturated solution makes the HAZ very fragile due to which its fatigue failure is reduced under combined loading.

Acknowledgment

Authors are happy to acknowledge the technical support of workshop staff of UCET especially Mr. Yasir and Mr. Asif Ali in specimen preparation.

References

[1] A. Wohler, "Fatigue crack growth under combined thermal cycling and mechanical loading", Int. J. Fatigue, vol. 29 pp. 1383–1390, 2007.

[2] Gerber, "Endurance limit and threshold stress intensity of die cast magnesium and aluminum alloys at elevated temperatures", Int. J. Fatigue, vol. 27, pp. 1076–1088, 2005.

[3] Ewing and Humfery, "Effects of microstructure and temperature on fatigue behavior of E319-T7 cast aluminum alloy in very long life cycles", Int. J. Fatigue, vol. 28, pp. 1566-1571, 2006.

[4] Griffith, "Ambient to high-temperature fracture toughness and cyclic fatigue behavior in Al-containing silicon carbide ceramics", Acta Materialia, vol. 51, pp. 6477-6491, 2003.

[5] Manson and Cofin, "The crack initiation mechanism of the forged Mg–Zn–Y–Zr alloy in the super-long fatigue life regime", Scripta Materialia, vol. 56, pp. 1-4, 2007.

[6] R.I Stephens, A. Fatemi, R. R. Stephens and H. O. Fuchs, "A Book of metal fatigue in engineering", John Wiley & Sons, Inc. vol. 2nd Edition, New York, 2001.

[7] N. Ranc, D. Wagner and P.C. Paris, "Study of Thermal Effects Associated with Crack propagation during very high cycle fatigue tests", Acta Materialia, vol. 56, pp. 4012–4021, 2008.

[8] Y. Akiniwa, N. Miyamoto, H. Tsuru and K. Tanaka "Notch effect on fatigue strength reduction of bearing steel in the very high cycle regime", Int. J. Fatigue, vol. 28, pp. 1555–1565, 2006.

[9] D. Leidermark, J. Moverare, K. Simonsson, S. Sjöström and S. Johansson, "Fatigue crack initiation in a notched single-crystal superalloy component", Procedia Engg., vol. 2, pp. 1067–1075, 2010.

[10] Lazzarin, R. Tovo and G. Meneghetti, "Fatigue crack initiation and propagation phases near notches in metals with low notch sensitivity", Int. J. Fatigue, vol. 19, pp. 647-657, 1997.

[11] M. Makkonen, "Notch size effects in the fatigue limit of steel", Int. J. Fatigue, vol. 25, pp. 17–26, 2003.

[12] T. Hsu and Z. Wang, "Fatigue crack initiation at notch root under compressive cyclic loading", Procedia Engg., vol. 2, pp. 91–100, 2010.

[13] I. Roth, M. Kübbeler, U. Krupp, H.J. Christ and C.-P. Fritzen, "Crack initiation and short crack growth in metastable austenitic stainless steel in the high cycle fatigue regime", Procedia Engg., vol. 2, pp. 941–948, 2010.

[14] R.E. Peterson, "Design Factors for stress concentration, parts 1 to 5", Machine design, February-July, 1951, Geometric stress concentration factors (BemdingExample) http://www.scribd.com/doc/6716719/Stress-Concentration-Factors-and-Notch-Sensitivity, Spotts Fig 2-12, Peterson.

[15] M. Cremer, M. Zimmermann and H. J. Christ, "High-frequency cyclic testing of welded aluminium alloy joints in the region of very high cycle fatigue (VHCF), Int. J. Fatigue, 2012.

[16] R. Yuan, J. J. Kruzic, X. F. Zhang, L. C. De Jonghe and R.O. Ritchie, "Ambient to high temperature fracture toughness and cyclic fatigue behavior in Al-containing silicon carbide ceramics", Acta Materialia, vol. 51, pp. 6477-6491, 2003.

[17] X. Zhu, A. Shyam, J. Jones, H. Mayer, J. Lasecki and J. Allison, "Effects of microstructure and temperature on fatigue behavior of

E319-T7 cast aluminum alloy in very long life cycles", Int. J. Fatigue, vol. 28, pp. 1566-1571, 2006.

[18] K.J. Miller and K. P. Zachariah, "Cumulative damage laws for fatigue crack initiation and stage-I propagation", J. Strain Analysis, vol. 12, pp. 262-270, 1977.

[19] S. Hassanifard and M. Zehsaz, "The effects of residual stresses on the fatigue life of 5083-O aluminum alloy spot welded joints," Procedia Engg., vol. 2, pp. 1077-1085, 2010.

[20] J. T. Burns, J. M. Larsen, and R. P. Gangloff, "Effect of initiation feature on microstructure scale fatigue crack propagation in Al–Zn–Mg– Cu", Int. J. Fatigue, vol. 42, pp. 104-121, 2012.

[21] H.T. Corten and T.J. Dolan, "Cumulative fatigue damage", Int. Conf. Fatigue of Metals Instn. Mech. Engrs, London, p. 235, 1956.

[22] Bui QuocThang et al. "Cumulative fatigue under stress controlled conditions", Trans. ASME., J. bas. Engg., p. 691, 1971.

[23] B.Q. Thang et al., "Cumulative fatigue under strain controlled conditions", Materials JMLSA, vol. 6, p. 718, 1971.

[24] H.J. Grover, "An observation concerning the cycle ratio in cumulative damage", Symp. on Fatigue in Aircraft Structures A.S.T.M., vol. 120, STP 274, 1960.

[25] B.F. Langer, "Fatigue failure from stress cycles of varying amplitude", Trans ASME, J. Appl. Mech. vol. 59, A-160, 1937.

[26] K. Störzel, T. Bruder and H. Hanselka, "Durability of welded aluminium extrusion profiles and aluminium sheets in vehicle structures", Int. J. Fatigue, vol. 34, pp. 76-85, 2012.

[27] M. Ullah, R.A. Pasha, G.Y. Chohan, Faisal. Qayyum, Numerical simulation and experimental verification of CMOD in CT specimens of TIG welded AA2219-T87, Arabian J. Sci. Engg., vol. 40, pp. 935-944, 2015.

[28] M. Ullah, C.S. Wu and M. Shah, In situ delta ferrite estimation and their effects on FCPR at different orientations of multipass shielded metal arc welded SS304L", J Manuf. Process, vol. 21, pp. 107-123, 2016.